Study on CO_2 Hydrate Formation Kinetics in Saline Water in the Presence of Low Concentrations of CH_4

Pranav Thoutam,[†] Sina Rezaei Gomari,*,[†] Antonin Chapoy,[‡] Faizan Ahmad,[†] and Meez Islam[†]

[†]Department of Chemical Engineering, School of Science Engineering and Design, Teesside University, Middlesbrough TS1 3BX, U.K.

[‡]Institute of Petroleum Engineering, Heriot-Watt University, Edinburgh EH14 4AS, U.K.

ABSTRACT: Gas-hydrate formation has numerous potential applications in the fields of water desalination, capturing greenhouse gases, and energy storage. Hydrogen bonds between water and guest gas are essential for hydrates to form, and their presence in any system is greatly influenced by the presence of either electrolytes or inhibitors in the liquid or impurities in the gas phase. This study considers CH_4 as a gaseous impurity in the gas stream employed to form hydrates. In developing gas-hydrate formation processes to serve multiple purposes, CO_2 hydrate formation experiments were conducted in the presence of another hydrate-forming gas, CH_4, at low concentrations in saline water. These experiments were conducted in both batch and stirred tank reactors in the presence of sodium dodecyl sulfate (SDS) as a kinetic additive at 3.5 MPa and 274.15 K, under isobaric and isothermal conditions. Gas loading was taken as the detection criterion for hydrate formation. It was observed that overall gas loading was hindered by more than 70% with the addition of salts after 2 days. The addition of CH_4 to the gas stream led to a further reduction of approximately 30% of gas loading in the batch reactor under quiescent conditions. However, the addition of 100 ppm of SDS improved the gas loading by recovering 34% of the loss observed in volumetric gas loading through the addition of salts and CH_4. The introduction of stirring improved the gas loading, and 64% of the loss was recovered through the addition of salts and CH_4 after 34 h. The investigation was continued further by substituting CH_4 with N_2, whereupon accelerated hydrate formation was observed.
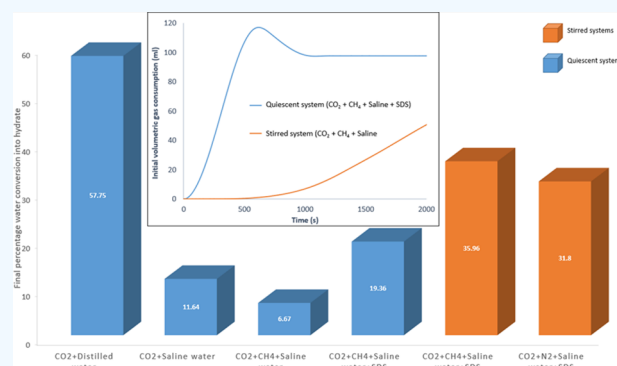
1. INTRODUCTION

Gas hydrates are crystalline compounds that are formed from a combination of single or mixed guest gases with water, generally in high-pressure and low-temperature conditions.[1] Despite being perceived as an issue to be solved in the transportation of natural gas, hydrate formation has attracted wide-ranging research interest since the discovery of its applications in energy storage and transportation, water desalination, and environmental sciences.[2−5] Due to its ability to selectively separate various gases depending upon thermodynamic conditions, hydrate formation has applications involving the separation of gases, such as CO_2 capture, the recovery of CH_4 from natural gas hydrates, and the storage and safe transportation of CH_4 using hydrates. However, the main drawbacks are thermodynamic (the heat of formation of hydrates) and physical [heterogeneous hydrate formation at the gas−liquid (g-l) interface], along with the need for high-pressure conditions and the unavailability of a reactor design for continuous hydrate formation.[6−9]

Even though, theoretically, hydrate formation is an exothermic process, its application for the intended purposes was in question due to the requirements of a high driving force. To improve the hydrate formation in terms of its yield and lowering the induction time, numerous studies were done

using different guest gases,[10−14] chemical additives such as kinetic and thermodynamic additives,[4,15−18] and physical interventions using stirring, porous media, nanotubes, nanoparticles, and hydrate formation in dry water and dry gel.[19−22] Despite being effective in improving the overall yield, porous media, microparticles, and nanoparticles could increase the process cost for requiring an additional filtration process to separate the particles from water.[19] Moreover, hydrate formation in the presence of nanoparticles could be effective in the presence of stirring. However, stirring in the aqueous phase with micro and nanoparticles could be excessively power-consuming because the liquid phase is highly viscous, whereas it is impossible in the presence of porous media.[19] Even it is stated that the energy requirement for stirring increases as the hydrate grows, making the overall aqueous-hydrate phase more viscous with time.[23] Hence, in this study, we have focused on the intervention that does not require additional separation processes and quiescent and stirred systems for the comparative analysis both in terms of initial kinetics and temporal yield.

With respect to desalination, CO_2-based hydrate formation comes under the category of freeze desalination where desalted water can be extracted from three steps of crystalline CO_2 hydrate formation, hydrate washing, and dissociation. This advanced freezing technique comes with an advantage of not demanding low temperatures while a disadvantage of requiring high-pressure conditions. The presence of CO_2 in the desalination process has the advantage of capturing acidic gases without requiring lower temperatures as much as conventional water freezing; however, high compressions are required, which, in turn, increase the energy consumption.[10] Through various experiments, salt removal rates of 60−80% have been observed in the first stage, which have been further improved up to 97% through later stages.[11,12] In addition to the physical interventions, various chemicals are added to the systems to improve the hydrate formation rates as well as yields. While kinetic additives improved the hydrate yield by encouraging the gas diffusivity in the aqueous phase without forming hydrates themselves, thermodynamic additives both improved the yield and minimized the induction time by forming hydrates.[24] As most of these thermodynamic additives are liquids, the effluent hydrate slurry requires further distillation to produce clean water. Especially, the chemical toxicity induced by these additives could potentially harm humans, making the effluent water not potable. Hence, the study considered only kinetic additives in the sensitivity analysis to keep the results suitable for the application in desalination. For its economic viability, availability, and efficiency in supporting hydrate formation, SDS is considered as the kinetic additive in our sensitivity studies.[25]

Gases such as propane, SF6, and HFC-forming hydrates can be used for desalination without requiring high compressions. However, their relative scarcity in nature or in industrial emissions would make their usage as the main hydrate expensive.[26] In addition, HFCs and CFCs are environmentally harmful and encouraging their production for use in desalination would lead to greater environmental concerns.[27] Moreover, the tiny and dendritic SII hydrates formed by propane and CFCs make separation from the brine solution extremely difficult. Even if they are separated, the brine samples trapped inside the hydrate structures are hard to be removed, lessening the practicability of the industrial hydrate-based desalination using these gases.[28] By addressing these issues, we have considered another easy hydrate former, CO_2, in this study. Instead of taking pure CO_2 for the study, which would be profoundly an ideal case, we have considered a 95% pure CO_2 with 5% CH_4 or N_2 in the gas stream. This is because the CO_2 produced by most of the CO_2 capture processes is not pure.[29] It also serves to understand the sensitivity of hydrate formation toward two gaseous impurities, distinguished by the nature of their solubilities in water.

Finally, the main aim of our study is to check the sensitivity of hydrate formation toward various chemical and physical interventions: quiescent, addition of CH_4 to CO_2 gas streams, addition of salt to water, addition of SDS, introduction of stirring, and the substitution of CH_4 with N_2. Hydrate formation studies under quiescent conditions were conducted for two days to record the volumetric gas consumption as the main observation. The kinetics observed from these systems were compared among themselves to derive conclusions over their hydrate formation sensitivities, which were further linked to physical and thermodynamic barriers that arise during the hydrate formation event. The objective is to also focus upon the effectiveness of stirring upon hydrate formation both initially and after few hours to derive conclusions where the stirring is effective.

2. EXPERIMENTAL SECTION

2.1. Materials. The experiments were conducted to study the kinetics of CO_2 hydrate formation in seawater with low concentrations of CH_4. CH_4 was chosen as a pollutant because combinations of CH_4 and CO_2 can be found naturally in the ores such as crude oil wells and natural gas ores.[30] Therefore, in addition to experiments with pure CO_2, a gas mixture of CO_2 and CH_4 was prepared with the composition shown in Table 1. The saline water was prepared according to the

Table 1. Gas and Saline Mixture Compositions

component	composition (mol %)	mixture
CO_2	95.085 ± 0.045	gas
CH_4	4.915 ± 0.045	gas
NaCl	0.87 ± 0.015	saline
Na_2SO_4	0.056 ± 0.001	saline
$MgCl_2$	0.018 ± 0.004	saline

seawater configuration mentioned by Nessim et al.[23] However, only three salts with major contributions to salinity were considered, whereas the rest were added to the molarity of NaCl. The composition of saline water is shown in Table 1. To improve the hydrate formation kinetics, 100 ppm of SDS was added to the liquid phase in the later experiments. The properties of the components are shown in Table 2.

Table 2. Materials Used in the Experiments

component	supplier	purity (%)
NaCl	Sigma-Aldrich	99.5 (mass %)
Na_2SO_4	BDH Laboratory Supplies, UK	99.0 (mass %)
$MgCl_2 \cdot 6H_2O$	Fisher Scientific, UK	99.5 (mass %)
CO_2	Air Products PLC, UK	99.995 (vol %)
SDS	Sigma-Aldrich	99.0 (mass %)
CH_4	BOC, Edinburgh	99.995 (vol %)

2.2. Operational Conditions. As high-temperature and low-pressure conditions generally favor hydrate formation, the system required either compression or refrigeration. In this study, a temperature just above the freezing point was chosen to keep the compression cost low.[31]

To check the hydrate-forming condition of the CH_4 and CO_2 mixture, predictions were generated using the model proposed by Chapoy et al. and are shown in Figure 1.[32] The provision of merely equilibrium pressure does not ensure hydrate formation as a driving force was needed, which was considered to be the difference between the experimental pressure and the equilibrium pressure.[33]

From the observations of Fakharian et al. on CO_2 hydrate formation, it was found that at pressures as high as 5.5 MPa the system was observed to have formed unstable CO_2 hydrates, whereas at 3.5 MPa, a stable CO_2 hydrate was formed.[34] It is also worth mentioning that the pressure of CH_4 hydrate dissociation to be 3.3 MPa, while it is 1.6 MPa for CO_2 hydrate at 274.15 K for sea water with a salinity of 3.5 wt %. Given these factors, the experiments were conducted at 3.5 MPa and 274.15 K to support hydrate formation while discouraging CH_4 hydrate formation.
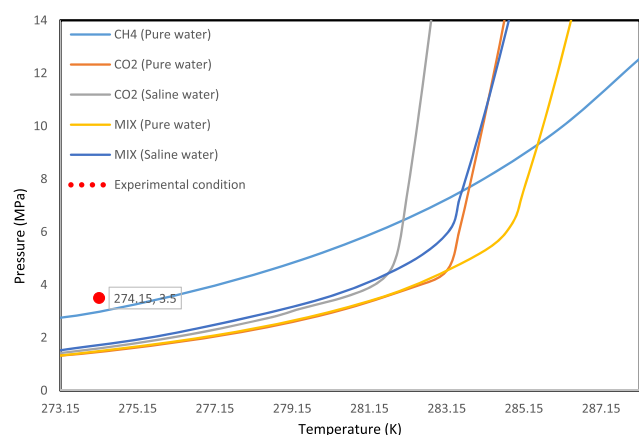
Figure 1. Equilibrium pressures of hydrates with gaseous pure components and mixtures.

2.3. Experimental Setup and Data Acquisition. An isothermal and isobaric system was considered for the experiments, where hydrate formation was detected from gas loading or volumetric gas consumption. Two jacketed-type reactor configurations were considered: a rocking cell reactor for quiescent systems and a stirred tank reactor.

A jacketed rocking cell with a volume of 377 mL was considered to conduct the quiescent hydrate formation studies. The rig was capable of performing a 180° pneumatic rocking, which was used at the time of gas dissolution. It had an operational temperature range of 203.15−323.15 K and a maximum pressure of 70 MPa. The coolant sent from a cryostat was circulated through the jacket of the rig to maintain the operational temperature. The cryostat was capable of maintaining the cell temperature within a range of 0.05 K. To further reduce heat transfer with the surroundings, the rig was insulated with a polystyrene board on its outside, whereas a plastic foam covered the connecting pipeline. A platinum resistance thermometer was positioned in the jacket to monitor the temperature during hydrate formation with an accuracy of ±0.05 K deviation. To measure pressure, a Quartzdyne pressure transducer was used. The pressure was measured with an accuracy of ±0.03 MPa. The temperature and pressure data were recorded on a PC, which was connected through an RS 232 serial port. Schematic diagrams of the experimental setup and the rocking cell reactor are given in Figure 2.

The reactor was connected to pressure and temperature transducers and the temperature probe and controller, which was attached to a refrigerator. A Quizix high-pressure syringe pump (Q6000-10K model) was attached to the reactor by means of a gas supply cell to maintain the system at the required pressure. The pump, temperature controller, and pressure and temperature transducers were attached to the data acquisition system. Detailed diagrams of the experimental setups for both systems are provided in Figure 2.

For all experiments, the mass liquid phase taken was 150 ± 0.2 g. Experiments were conducted in two stages: dissolution and hydrate formation. In the dissolution phase, the system was maintained at 285.15 K and 3.5 MPa to make sure that there was no hydrate formation. For the rocking cell reactor, the system was put into the continuous rocking mode while in the dissolution phase. The internal volumes of the rocking cell and stirred tank reactors were 377 and 525 mL, respectively. The stirred tank reactor consisted of a jacketed-type rig with a volume of 525 mL. The rig was set with a magnetic stirrer

having an adjustable rotational speed that was measured with respect to the viscosity of the test fluid. The maximum allowable pressure was 69 MPa, whereas it had an operating temperature range of 253.15−348.15 K. As in the rocking cell reactor, the coolant from the cryostat was sent to the jacket to control and maintain the temperature. A thermocouple with an accuracy of 0.1 K was placed inside the reactor to monitor the operational temperature. The pressure was monitored using a Quartzdyne pressure transducer, which had an accuracy of ±0.015 MPa. To reduce further heat loss, the rig was kept in another stainless steel container. To be able to monitor temperature and pressure trends, the thermocouple and pressure transducers were connected to a PC, which also collected torque data. Figure 1c shows a schematic diagram of the stirred tank reactor.

A Quizix high-pressure syringe pump (Q6000-10K model) was attached to the reactor by means of a gas supply cell to maintain the system at the required pressure conditions. Before starting each experiment, the reactors were cleaned and vacuumed. The experiments were conducted in two stages: dissolution and hydrate formation. In the dissolution phase, the system was maintained at 285 K and 3.5 MPa to make sure that no hydrate formation occurred. For the rocking cell reactor, the system was put into the continuous rocking mode while in the dissolution phase.

A stirring speed of 360 rpm was set throughout the experiment for the hydrate formation under stirring conditions. Generally, gas dissolution took approximately 40−60 min. Once dissolution was completed in the rocking reactor, rocking was stopped, and the reactor was set horizontally so as to increase the gas−liquid interface. The temperature of the system was set to 274.15 K, and the initial volumetric consumption at this stage was set to zero. Generally, experiments were stopped after a time period of 3 days, unless the system had reached a long-term quasisteady state in terms of volumetric gas consumption before that. The volumetric gas consumption and temperature and pressure fluctuations were recorded and analyzed to check the kinetics of hydrate formation. In this study, a total of five experiments were conducted, as listed in Table 3. To check the reproducibility of these observations, the experiments were repeated once, which produced similar results. Once the gas consumption data from the experiments was collected, the volume of gas involved in hydrate formation was calculated by eliminating the share of volumetric gas consumption due to the gas contraction and gas dissolution during the temperature drop as well as the volume consumption contributed by the contraction of the hydrate−water phase during the hydrate formation. This process was explained in the Discussion section.

3. RESULTS AND DISCUSSION

In this section, the profiles of volumetric gas consumption during hydrate formation in the experiments are discussed. As explained previously, the value of volumetric gas consumption was set to zero before the experimental temperature was changed to 274.15 K. Hence, the values of volumetric gas consumption given are the result of the following four phenomena that subsequently occur: (1) A shift in the vapor−liquid equilibrium of the gas and liquid (further dissolution of gas into the liquid); (2) contraction of the gas phase due to the temperature drop; (3) hydrate formation; and (4) contraction of the hydrate−liquid phase due to the formation of hydrates with higher density.
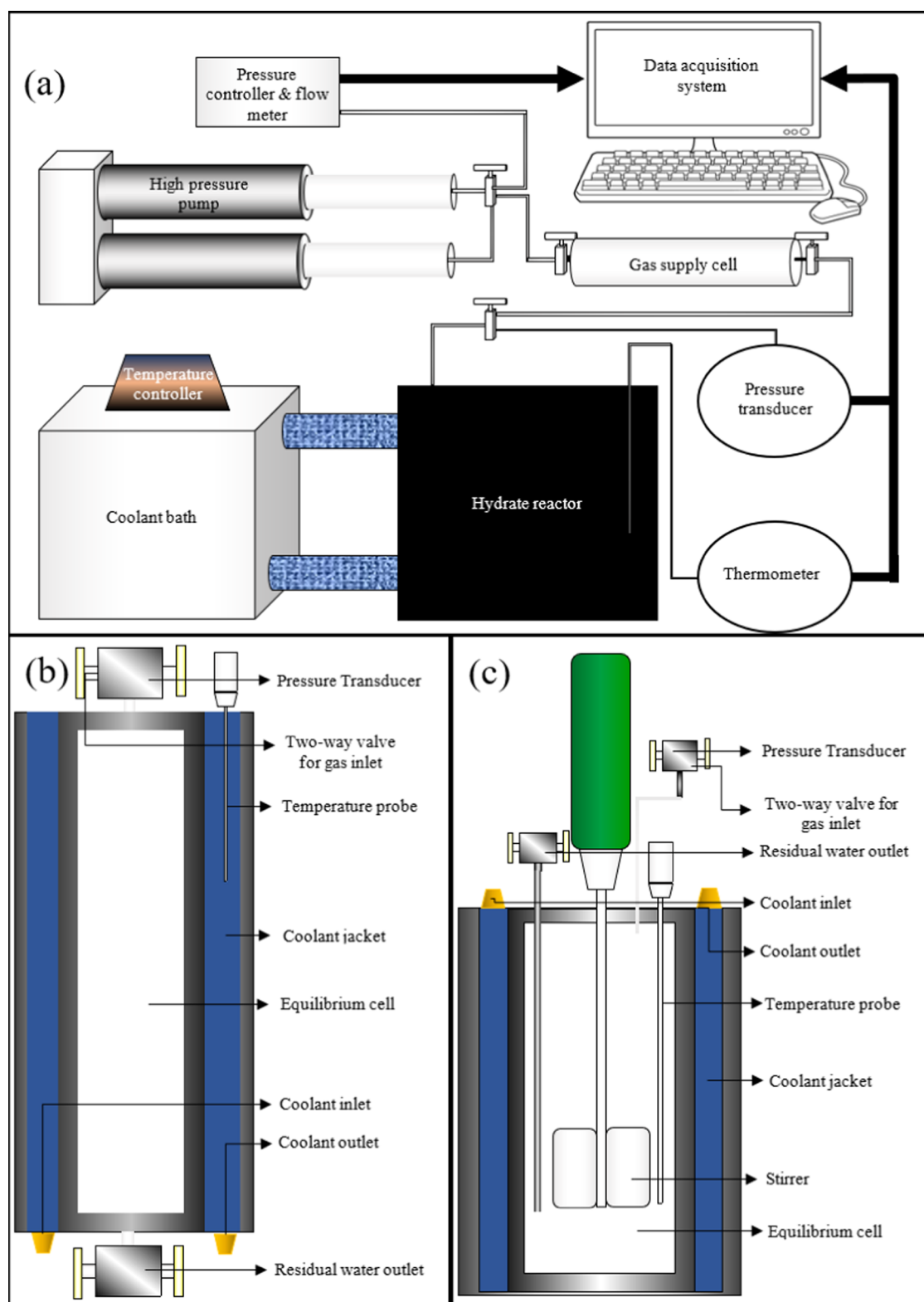
Figure 2. Experimental setup configurations: (a) with the rocking cell reactor, (b) for quiescent conditions, and (c) stirred tank reactor.

The experiments were conducted for two to three days depending upon the status of volumetric gas consumption. However, all of the quiescent systems were compared for a time period of two days, whereas this was shortened to 34 h when comparing the stirring experiments due to the premature cessation of stirring caused by excessive hydrate formation in the system. The system with CO_2 and distilled water in

quiescent conditions, which was discussed in a previous study, was considered as the base case against which the rest of the systems were compared.[35]

3.1. Experimental Observations. Figure 3 shows how the presence of salt, CH_4, and 100 ppm of SDS in the system affected the kinetics of hydrate formation in the systems. For the base case of CO_2 and distilled water, a total of 542 mL of

Table 3. List of Experiments Conducted in This Study

| exp. no.	system	physical configuration	experimental setup
1	CO_2 + distilled water	quiescent	rocking cell
2	CO_2 + saline water	quiescent	rocking cell
3	CO_2 + CH_4 + saline water	quiescent	rocking cell
4	CO_2 + CH_4 + saline water + SDS	quiescent	rocking cell
5	CO_2 + CH_4 + saline water + SDS	stirring	stirred tank
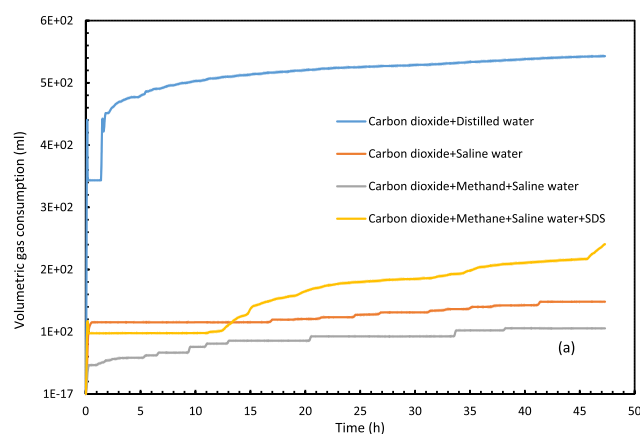
Figure 3. Volumetric gas consumption by quiescent systems.

gas consumption was observed, out of which 43 mL was the contribution of gas contraction after the temperature dropped from 285.15 to 274.15 K. It is observed that the addition of salts had a detrimental effect on hydrate formation. At the end of the second day, the volumetric gas consumption was observed to be 148 mL, which was almost 73% less than in the previous case. In the next experiment, a 95 mol % CO_2 + 5 mol % CH_4 stream was used. For this mixture, a further 29% fall in gas consumption compared to the previous case was observed. In the literature, the effect of SDS has been proven to enhance hydrate formation by decreasing the interfacial tension within the liquid regime and hence improve the diffusion of gas to the sites of hydrate formation.[36] In support of such observations, when 100 ppm of SDS was added to the system, gas consumption was increased to 2.28 times the value observed in the CO_2 + CH_4 system in saline water. This is equivalent to 34% of the volumetric gas consumption lost during the addition of salts and CH_4 to the system by the end of the second day. This value was further increased to 52% at the end of the next day.

When comparing gas loading at the end of 34 h, the reduction in the volumetric gas consumption with the addition of salts was 78%. Addition of CH_4 to the system further reduced the volumetric gas consumption by 38%. Addition of SDS to the system at this stage recovered 27% of the gas loading that was lost during the addition of salts and CH_4.

3.2. Barriers toward Hydrate Formation. There are three main factors that can interfere with hydrate formation: the physical barrier, heat generation, and heat distribution. The existing hydrate layer represents a physical barrier to further gas dissolution into the system, hence hindering further hydrate formation. Heat generation occurs because hydrate formation is exothermic in nature. This can be a potential hindrance to hydrate formation as the process is highly sensitive to rises in temperature. Heat distribution is a major hindrance to hydrate formation, especially in quiescent

systems, when localized high-temperature regimes occur. This made the hydrate formation sporadic, especially after the first exponential volume consumption, where the cycles of hydrate formation and dissociations or overall hydrate formation with slower kinetics were seen for extended periods of time. The localization of heat can be discouraged by introducing stirring into the system. However, in our experiments, a temperature rise of 4 °C was observed within the stirred tank reactor during the exponential phase of hydrate formation, resulting in a drop in gas consumption. At the end of the experiment, the stirred case was observed to have recovered 65% of the volumetric gas consumption that was lost due to the addition of the salts and CH_4 to the system. This recovery is more than 2.31 times that found in the quiescent system. Figure 4 illustrates how the introduction of stirring improved the kinetics of hydrate formation.
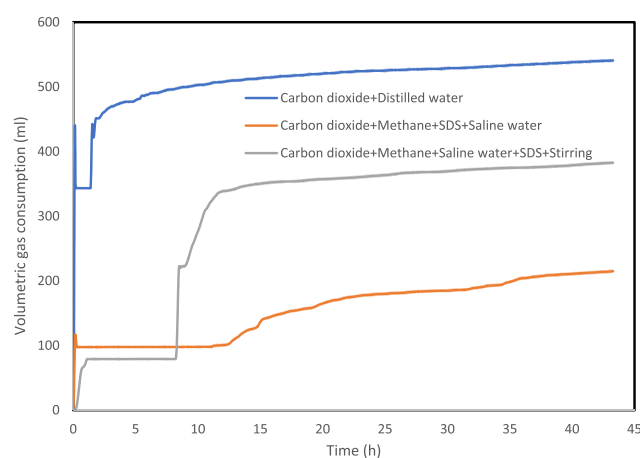
Figure 4. Comparison of volumetric gas consumption in the systems involving SDS with and without stirring with the base case of CO_2 + distilled water.

In experiments using CO_2 and CH_4, Long and Sloan and Takeya et al. observed that hydrate formation always started at the gas–liquid interface at the wall and propagated either along the wall or along the gas–liquid interface, depending upon the choice of guest gas and the presence of kinetic additives in the system. When hydrates are propagated along the gas–liquid interface, despite the porous nature of hydrates, it is more probable to affect the further dissolution of CO_2 into the solution.[37,38] In the present experiments with both quiescent and stirred systems, it was observed that hydrate formation occurred and propagated along the reactor wall instead of at the gas–liquid interface. Hence, the occurrence of physical interference can be ruled out. This observation supports the suggestion by Ribeiro et al. and Takeya et al. that hydrate formation with gases of low solubility occurs at the gas–liquid interface due to the high availability of dissolved gas there.[39,40] Moreover, CO_2 is a highly soluble gas, which forms hydrates along the reactor walls, as is evidently the case here. However, from the volumetric gas consumption profiles generated by the quiescent systems, it is clear that the process of hydrate formation was not continuous but sporadic. There were numerous periods of time during which the gas consumption trends showed a quasidormant state with no or minimal hydrate formation. With the g-l interface free for the mass transfer of gas into the liquid without any hindrance offered by the hydrate, the only possible explanation for this is the lack of

the dissipation of heat generated at the sites of hydrate formation. The effect of heat generation has been considerably high for the systems with high hydrate formations, where temperature rises of three to four degrees were observed, resulting in a reduction of volumetric gas consumption.

3.3. Gas Consumption toward Hydrate Formation. It is important to note that the gas consumption that has been discussed so far is the amount of gas injected into the reactor when the temperature reached 274.15 K. Apart from hydrate formation, this gas was consumed to compensate for the contraction of the gaseous phase due to the temperature drop and the contraction of the hydrate−liquid phase due to the density difference between the water-rich liquid phase and the hydrate phase and also to solve extra gas into the system during the temperature drop. The excess gas required to compensate for the contraction of gas is calculated using eq 1, yielding values of 37.67 mL for the quiescent system and 62.24 mL for the stirred system.

$$V_{ex} = \left(\left[\frac{ZRT}{P} \right]_T - \left[\frac{ZRT}{P} \right]_{T_o} \right) \times V_g \tag{1}$$

where V_{ex} is the excess volume needed to compensate for the contraction of the gaseous phase, Z is the compressibility factor of the gas/gas mixture, R is the universal gas constant, T is the temperature, T_0 is the initial temperature, P is the pressure, and V_g is the total volume of the gaseous phase.

Before starting the experiment, the systems were given sufficient time to reach vapor−liquid equilibrium. When the temperature was set to 1 °C, the dissolution of further gas into the liquid phase occurred before the temperature conditions suitable for hydrate formation had been reached. Hence, the excess gas dissolution is assumed to have happened without the presence of hydrates. A modified Duan and Sun model is employed to calculate the excess volumetric gas consumption contributed by dissolution of gas into liquid during the temperature shift.[41] When applying the model to calculate the gas dissolution to systems with a mixture of CO_2 and CH_4, a modified fugacity coefficient is used, which has been taken from Ricaurte et al.[42] The volumes contributing to the changes in gas dissolution in the system were calculated to be 0.392 mL for the CH_4 + CO_2 system and 0.386 mL for the pure CO_2 system in saline water. For the CO_2 and distilled water system, the excess volume due to dissolution was 0.389 mL.

For the calculation of excess volume due to the contraction of the hydrate−liquid phase due to the formation of hydrates, an iterative process was chosen. The density of hydrates was taken to be 1.10 g/cm³, whereas the density of saline water was chosen to be 1.03 g/cm³.[3,43] For the calculation of the number of moles of water converted into hydrates given the s1 structure of hydrate formation, the stoichiometric ratio of water to gas of 5.75:1 was used.[22,44] Initially, the residual volumetric gas consumption values were derived by subtracting the excess volumes of gas contraction and dissolution. Volumes of water and hydrates were calculated by assuming that the total residual gas consumption was used in the formation of hydrates. The excess volumes were subtracted from the previous residual volume consumption values to derive new residual volume consumption amounts. After two iterations, the residual values were narrowed down to be less than 0.002. After subtracting all of these excess volumes, the volume of gas that participated in hydrate formation at the end of 34 h could be calculated, and the results are given in Table 4.

Table 4. Volume of Gas Participating in Hydrate Formation after 34 h

experiment number	experiment	volume of gas used for hydrates (mL)
1	CO_2 + distilled water	491.57
2	CO_2 + saline water	99.08
3	CO_2 + CH_4 + saline water	56.83
4	CO_2 + CH_4 + saline water + SDS	164.81
5	CO_2 + CH_4 + saline water + SDS	306.08
6	CO_2 + N_2 + saline water + SDS	213.22 (after 21 h)

The values given in Table 4 show the extent of hydrate formation at the end of the 34 h periods of the experiments. Values of the efficiency of the physical interventions and chemical additives in either enhancing or reducing hydrate formation were calculated. At the end of 34 h, the addition of salts reduced hydrate formation by 80%. This value was further reduced by 43% with the introduction of 5 mol % CH_4. With the addition of 100 ppm of SDS, 25% of the volumetric loss in hydrate formation due to the addition of salts and 5 mol % CH_4 was recovered. When stirring was introduced, the recovery level rose to 57%, which is 2.3% higher than in the quiescent case. From these values, it is obvious that the contributors for volume consumptions were quantitively different for different systems.

3.4. Initial Hydrate Formation Kinetics. Even though introduction of stirring was beneficial for hydrate formation by improving the heat distribution throughout the reactor, it was seen to have reduced heterogeneous hydrate formation. Moreover, instantaneous heterogeneous hydrate formation was observed in all of the quiescent experiments. This can be seen from the results for gas consumption a few minutes after the temperature was set to 1 °C. However, this exponential increase in gas consumption was not seen in stirred systems. To check this observation, volumetric gas consumption profiles were plotted for the first 500 min and compared, as shown in Figure 5. At 480 s, the volumetric gas consumption of the quiescent CO_2 + distilled water system reached its local maximum (440 mL), which then decreased due to the temperature rise, marking the end of exponential hydrate formation. Hence, the first 500 s was chosen for the comparison of exponential hydrate formation rates. The absence of exponential hydrate formation might have been
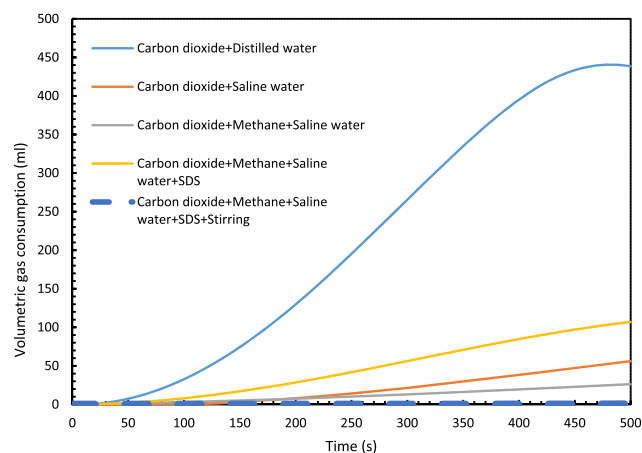

Figure 5. Volumetric gas consumption within the first 500 s of the experiment.

caused by the attrition of the nuclei or turbulence along the reactor wall instigated by the stirring, which might have decreased the static interaction between the wall and the liquid phase. Even though the stirring discouraged exponential hydrate formation in the initial stages, it was observed that overall the hydrate formation occurred mostly near the wall.

3.5. Comparison between CH_4 and N_2. Experiment 5 was repeated by substituting CH_4 with N_2 to check the effect of a gaseous impurity with a lesser solubility in the system.[10] This experiment was stopped after 21 h, and the values noted were compared with the results from experiment 5. Studies such as that by Ahmad and Gersen suggest that the extent of the dissolution of CO_2 is greatly reduced with the addition of N_2 and CH_4.[1] Moreover, in the presence of hydrates, the extent of CH_4 dissolution into water increases when using a mixture of CO_2 and CH_4 in the guest gas phase.[16] With the presence of more gaseous impurities in the liquid phase, their interference with ongoing hydrate formation may increase, causing overall hydrate formation to decelerate.

In our experiments, smoother and more exponential hydrate growth was observed in the experiment with N_2 rather than CH_4, as can be seen in Figure 6. This suggests that the hydrate
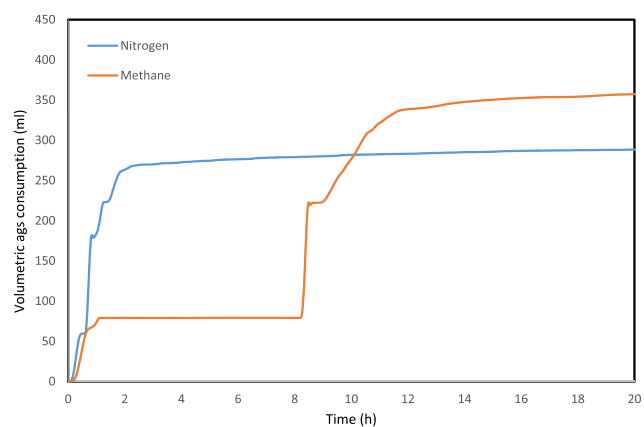

Figure 6. Comparison of CO_2 gas consumption in the presence of 5 mol % N_2 and 5 mol % CH_4 during hydrate formation.

formation when taking N_2 as a gaseous impurity is faster than CH_4 as the impurity. However, the overall yield was observed to be higher in the case of CH_4. This might be due to the premature cessation of stirring due to the presence of high volumes of hydrates in the system in the case of N_2. Even though its overall yield was lower, the consumption of 250 mL of gas was reached in the N_2 system within two hours, whereas it took approximately 10 h for the $CO_2 + CH_4$ system to consume that amount of gas, indicating faster hydrate formation in the $CO_2 + N_2$ system during the stirring process. Due to the unavailability of a temperature probe within the solution, and also the higher probability of localized elevated temperature regimes, minor temperature fluctuations in the quiescent systems were not captured. However, the temperature fluctuations were accurately recorded in the stirred systems. Figures 7 and 8 show the effect of temperature fluctuations on hydrate formation in the $CO_2 + CH_4$ and $CO_2 + N_2$ systems, respectively. These fluctuations were higher in the periods of exponential hydrate growth, indicating the exothermic behavior of the hydrate. In addition, plunges in hydrate growths were observed to be proportional to the temperature rise, showing the sensitivity of hydrate formation
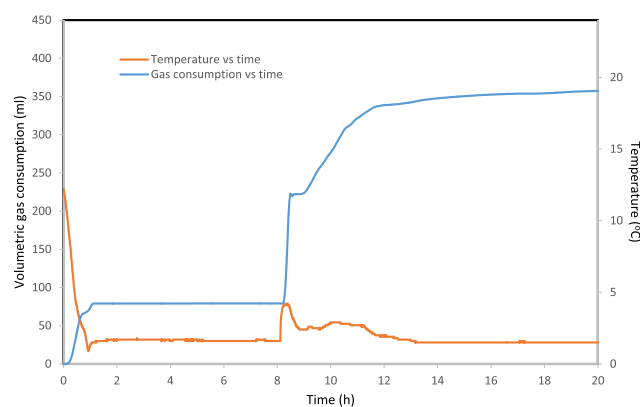

Figure 7. CO_2 gas consumption comparison against temperature in the $CO_2 + CH_4$ system during hydrate formation.
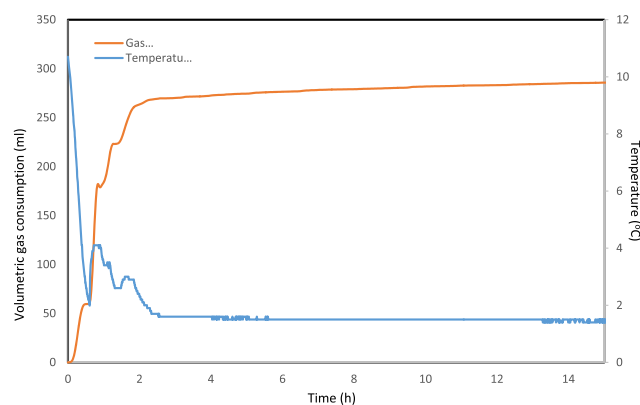

Figure 8. CO_2 gas consumption comparison against temperature in the $CO_2 + N_2$ system during hydrate formation.

to temperature. This suggests that heat absorbers are needed within the system to improve overall hydrate kinetics and yields.[18,19] Additional hydrate separation requirements caused by these absorbers discourage them to be used in the system. However, usage of better hydrate promoters combined with the continuous removal of hydrates could help the system to improve its overall yield without requiring heat absorbers. This needs cost analysis in between the hydrate−absorber separation process compared against the energy demand of continuous hydrate removal. Since the hydrates have formed with defined boundaries and considerable strength, unlike the hydrates of propane and CFCs, separation of these hydrates from brine was easy.

3.6. Water Conversion into Hydrates. To further investigate hydrate yields, values of the total conversion of water into hydrates were calculated for the s1 structure of CO_2 hydrates. The results are listed in terms of percentage conversion. As with the gas consumption results, the lowest water-to-hydrate conversion was found in experiment 3 with a total conversion of approximately 7%. The highest conversion was found in experiment 1 at approximately 58%. Among the saline systems, the system with stirring and 100 ppm of SDS (experiment 5) gave a total conversion of 35%. In the case of $CO_2 + N_2$, the value was approximately 32%. The water conversion results are shown in Table 5.

4. CONCLUSIONS

The kinetics of CO_2 hydrate formation has been studied under various inhibiting and supporting conditions to quantitatively

Table 5. Volume of Gas Participating in Hydrate Formation after 34 h

experiment number	experiment	molar percentage of water conversion
1	CO_2 + distilled water	57.75
2	CO_2 + saline water	11.64
3	CO_2 + CH_4 + saline water	6.67
4	CO_2 + CH_4 + saline water + SDS	19.36
5	CO_2 + CH_4 + saline water + SDS	35.96
6	CO_2 + N_2 + saline water + SDS	31.80

check its sensitivity toward these conditions. A total of five experiments were conducted, the first experiment of which used the basic conditions of having only water and pure CO_2 gas in a quiescent system. The impact of electrolytes and gaseous impurities on CO_2 hydrate formation was studied in the next two experiments, whereas a kinetic additive such as SDS and a physical intervention were introduced in the final two.

Experimental observations of volumetric gaseous consumption were used to measure the formation of hydrates by calculating the level of gas conversion. It was found that hydrate formation was greatly reduced by the introduction of salts. A further reduction resulted from the addition of small amounts of methane to the gas stream, making methane composition in the gaseous mixture up to 5 mol % of the resultant gaseous mixture.

Since CO_2 hydrate formation did not occur at the gas–liquid interface, there was no physical barrier toward the dissolution of gas during hydrate formation. Considerable temperature fluctuations acted as thermodynamic barriers in both quiescent and stirred systems. However, stirring helped in dissipating heat throughout the reactor, which resulted in higher overall hydrate yields as well as in smoother volumetric gas consumption profiles.

Despite improving the eventual hydrate yields, initial heterogeneous hydrate formation was observed to be hindered in the stirred systems. This suggests that if an effective heat removal technique is provided, quiescent systems could be more productive than stirred systems in terms of both formation kinetics and yields at lower operational costs. This observation suggests that if an effective continuous removal of hydrate is provided without disturbing the static liquid water interactions, the kinetics of hydrate formation can be higher in unstirred systems, making the process economic and efficient.

■ AUTHOR INFORMATION

Corresponding Author
*E-mail: s.rezaei-gomari@tees.ac.uk.

ORCID ⊙
Sina Rezaei Gomari: 0000-0001-7317-0690
Antonin Chapoy: 0000-0002-1368-5091
Meez Islam: 0000-0002-6858-6963

Notes
The authors declare no competing financial interest.

■ ACKNOWLEDGMENTS

■ REFERENCES

(1) Ahmad, M.; Gersen, S. Water solubility in CO_2 mixtures: Experimental and modelling investigation. *Energy Procedia* **2014**, *63*, 2402−11.
(2) Aliev, A. M.; Yusifov, R. Y.; Kuliev, A. R.; Yusifov, Y. G. Method of gas hydrate formation for evaluation of water desalination. *Russ. J. Appl. Chem.* **2008**, *81*, 588−591.
(3) Aya, I.; Yamane, K.; Nariai, H. Solubility of CO_2 and density of CO_2 hydrate at 30 MPa. *Energy* **1997**, *22*, 263−271.
(4) Babu, P.; Linga, P.; Kumar, R.; Englezos, P. A review of the hydrate based gas separation (HBGS) process for carbon dioxide pre-combustion capture. *Energy* **2015**, *85*, 261−279.
(5) Babu, P.; Nambiar, A.; He, T.; Karimi, I. A.; Lee, J. D.; Englezos, P.; Linga, P. A Review of Clathrate Hydrate Based Desalination to Strengthen Energy−Water Nexus. *ACS Sustainable Chem. Eng.* **2018**, *6*, 8093−8107.
(6) Fan, S.; Yang, L.; Lang, X.; Wang, Y.; Xie, D. Kinetics and thermal analysis of methane hydrate formation in aluminum foam. *Chem. Eng. Sci.* **2012**, *82*, 185−193.
(7) Fosbøl, P.; von Solms, N.; Gladis, A.; Thomsen, K.; Kontogeorgis, G. M. Methods and Modelling for Post-combustion CO_2 Capture. *Process Systems and Materials for CO2 Capture: Modelling, Design, Control and Integration*; Wiley, 2017; pp 243.
(8) Gayet, P.; Dicharry, C.; Marion, G.; Graciaa, A.; Lachaise, J.; Nesterov, A. Experimental determination of methane hydrate dissociation curve up to 55 MPa by using a small amount of surfactant as hydrate promoter. *Chem. Eng. Sci.* **2005**, *60*, 5751−5758.
(9) Hand, J. H.; Katz, D. L.; Verma, V. K. Review of Gas Hydrates with Implication for Ocean Sediments. *Natural Gases in Marine Sediments*; Springer: Boston, MA, 1974; pp 179−194.
(10) Kolev, N. I. Solubility of O_2, N_2, H_2 and CO_2 in Water. *Multiphase Flow Dynamics*; Springer: Berlin, Heidelberg, 2011; Vol. 4.
(11) Kumar, A.; Sakpal, T.; Linga, P.; Kumar, R. Influence of contact medium and surfactants on carbon dioxide clathrate hydrate kinetics. *Fuel* **2013**, *105*, 664−671.
(12) Lee, D.; Lee, Y.; Lee, S.; Seo, Y. Accurate measurement of phase equilibria and dissociation enthalpies of HFC-134a hydrates in the presence of NaCl for potential application in desalination. *Korean J. Chem. Eng.* **2016**, *33*, 1425−1430.
(13) Li, X. S.; Xu, C. G.; Chen, Z. Y.; Wu, H. J. Tetra-n-butyl ammonium bromide semi-clathrate hydrate process for post-combustion capture of carbon dioxide in the presence of dodecyl trimethyl ammonium chloride. *Energy* **2010**, *35*, 3902−3908.
(14) Li, X. S.; Xia, Z. M.; Chen, Z. Y.; Wu, H. J. Precombustion capture of carbon dioxide and hydrogen with a one-stage hydrate/membrane process in the presence of tetra-n-butylammonium bromide (TBAB). *Energy Fuels* **2011**, *25*, 1302−1309.
(15) Li, Z.; Zhong, D. L.; Lu, Y. Y.; Yan, J.; Zou, Z. L. Preferential enclathration of CO_2 into tetra-n-butyl phosphonium bromide semiclathrate hydrate in moderate operating conditions: Application for CO_2 capture from shale gas. *Appl. Energy* **2017**, *199*, 370−381.
(16) Li, Z.; Wang, X.; Xue, Q.; Liu, M. Calculation for Solubility of Methane and Carbon Dioxide in Water in Presence of Hydrate, *The 28th International Ocean and Polar Engineering Conference*; International Society of Offshore and Polar Engineers: Sapporo, Japan, 2018.
(17) Linga, P.; Kumar, R.; Englezos, P. The clathrate hydrate process for post and pre-combustion capture of carbon dioxide. *J. Hazard. Mater.* **2007**, *149*, 625−629.
(18) Linga, P.; Haligva, C.; Nam, S. C.; Ripmeester, J. A.; Englezos, P. Gas hydrate formation in a variable volume bed of silica sand particles. *Energy Fuels* **2009**, *23*, 5496−5507.
(19) Linga, P.; Clarke, M. A. A review of reactor designs and materials employed for increasing the rate of gas hydrate formation. *Energy Fuels* **2016**, *31*, 1−13.
(20) Long, J. P.; Sloan, E. D. Hydrates in the ocean and evidence for the location of hydrate formation. *Int. J. Thermophys.* **1996**, *17*, 1−13.
(21) Max, M. D.; Pellenbarg, R. E.; US Secretary of Navy Desalination through Methane Hydrate. US5,873,2621999.

(22) McMullan, R. K.; Jeffrey, G. A. Polyhedral clathrate hydrates. IX. Structure of ethylene oxide hydrate. *J. Chem. Phys.* **1965**, *42*, 2725−2732.

(23) Nessim, R. B.; Tadros, H. R.; Taleb, A. E. A.; Moawad, M. N. Chemistry of the Egyptian Mediterranean coastal waters. *Egypt. J. Aquat. Res.* **2015**, *41*, 1−10.

(24) Dashti, H.; Yew, L. Z.; Lou, X. Recent advances in gas hydrate-based CO_2 capture. *J. Nat. Gas Sci. Eng.* **2015**, *23*, 195−207.

(25) Ganji, H.; Manteghian, M.; Omidkhah, M. R.; Mofrad, H. R. Effect of different surfactants on methane hydrate formation rate, stability and storage capacity. *Fuel* **2007**, *86*, 434−441.

(26) Nohra, M.; Woo, T. K.; Alavi, S.; Ripmeester, J. A. Molecular dynamics Gibbs free energy calculations for CO2 capture and storage in structure I clathrate hydrates in the presence of SO2, CH4, N2, and H2S impurities. *J. Chem. Thermodyn.* **2012**, *44*, 5−12.

(27) Pasieka, J.; Coulombe, S.; Servio, P. Investigating the effects of hydrophobic and hydrophilic multi-wall carbon nanotubes on methane hydrate growth kinetics. *Chem. Eng. Sci.* **2013**, *104*, 998− 1002.

(28) Miller, J. E. *Sandia National Labs Unlimited Release Report SAND-2003-0800*; Review of Water Resources and Desalination Technologies, 2003.

(29) Chapoy, A.; Burgass, R.; Tohidi, B.; Austell, J. M.; Eickhoff, C. Effect of common impurities on the phase behavior of carbon-dioxide-rich systems: Minimizing the risk of hydrate formation and two-phase flow. *SPE J.* **2011**, *16*, 921−930.

(30) Van Denderen, M.; Ineke, E.; Golombok, M. CO_2 removal from contaminated natural gas mixtures by hydrate formation. *Ind. Eng. Chem. Res.* **2009**, *48*, 5802−5807.

(31) Tajima, H.; Yamasaki, A.; Kiyono, F. Energy consumption estimation for greenhouse gas separation processes by clathrate hydrate formation. *Energy* **2004**, *29*, 1713−1729.

(32) Chapoy, A.; Burgass, R.; Tohidi, B.; Alsiyabi, I. Hydrate and phase behavior modeling in CO2-rich pipelines. *J. Chem. Eng. Data* **2014**, *60*, 447−453.

(33) Kashchiev, D.; Firoozabadi, A. Driving force for crystallization of gas hydrates. *J. Cryst. Growth* **2002**, *241*, 220−230.

(34) Fakharian, H.; Ganji, H.; Naderifar, A. Saline produced water treatment using gas hydrates. *J. Environ. Chem. Eng.* **2017**, *5*, 4269− 4273.

(35) Thoutam, P.; Rezaei Gomari, S.; Ahmad, F.; Islam, M. Comparative Analysis of Hydrate Nucleation for Methane and Carbon Dioxide. *Molecules* **2019**, *24*, 1055.

(36) Seo, Y. T.; Moudrakovski, I. L.; Ripmeester, J. A.; Lee, J. W.; Lee, H. Efficient recovery of CO2 from flue gas by clathrate hydrate formation in porous silica gels. *Environ. Sci. Technol.* **2005**, *39*, 2315− 2319.

(37) Tam, S. S.; Stanton, M. E.; Ghose, S.; Deppe, G.; Spencer, D. F.; Currier, R. P.; Young, J. S.; Anderson, G. K.; Le, L. A.; Devlin, D. J. A High-Pressure Carbon Dioxide Separation Process for IGCC Plants, *First National Conference on Carbon Sequestration*; Washington DC, 2001; pp 14−17.

(38) Zhong, Y.; Rogers, R. E. Surfactant effects on gas hydrate formation. *Chem. Eng. Sci.* **2000**, *55*, 4175−4187.

(39) Ribeiro, C. P., Jr.; Lage, P. L. Modelling of hydrate formation kinetics: State-of-the-art and future directions. *Chem. Eng. Sci.* **2008**, *63*, 2007−2034.

(40) Takeya, S.; Hori, A.; Hondoh, T.; Uchida, T. Freezing-memory effect of water on nucleation of CO2 hydrate crystals. *J. Phys. Chem. B* **2000**, *104*, 4164−4168.

(41) Duan, Z.; Sun, R. An improved model calculating CO2 solubility in pure water and aqueous NaCl solutions from 273 to 533 K and from 0 to 2000 bar. *Chem. Geol.* **2003**, *193*, 257−271.

(42) Ricaurte, M.; Torre, J. P.; Asbai, A.; Broseta, D.; Dicharry, C. Experimental data, modeling, and correlation of carbon dioxide solubility in aqueous solutions containing low concentrations of clathrate hydrate promoters: application to $CO_2−CH_4$ gas mixtures. *Ind. Eng. Chem. Res.* **2012**, *51*, 3157−3169.

(43) Serway, R. A.; Jewett, J. W. *Physics for Scientists and Engineers with Modern Physics*; Cengage Learning, 2018.

(44) Yoshioki, S. Identification of a mechanism of transformation of clathrate hydrate structures I to II or H. *J. Mol. Graphics Modell.* **2012**, *37*, 39−48.